Edisto Inlet as a sentinel for the Late Holocene environmental changes over the Ross Sea: insights from foraminifera turnover events

Giacomo Galli[1,2], Katrine Elnegaard Hansen[3], Caterina Morigi[2], Alessio di Roberto[4], Federico Giglio[5], Patrizia Giordano[5] and Karen Gariboldi[2]

[1]Department of Environmental Sciences, Informatics and Statistics, Ca' Foscari University of Venice, Via Torino 155, 30172 Venice, Italy
[2]Department of Earth Sciences, University of Pisa, Via Santa Maria 53, 56126, Pisa, Italy
[3]Department of Near Surface Land and Marine Geology, The Geological Survey of Denmark and Greenland (GEUS), 8000 Aarhus C, Aarhus, Denmark
[4]National Institute of Geophyisics and Vulcanology (INGV), Section of Pisa, Via Cesare Battisti 53, 56125, Pisa, Italy
[5]National Institute of Polar Sciences (CNR-ISP), Section of Bologna, Via Piero Gobbetti 101, 40129, Bologna, Italy

Correspondence to: Giacomo Galli (giacomo.galli@unive.it)

Abstract. Identifying marine environmental changes is important to understand the processes that govern the Earth's climate system and its interacting components. Microfossil assemblages are one of the most used paleoenvironmental tracers, ~~being able to connect changes in~~with their community composition ~~to~~ responding to changes in the physiochemical characteristics of the environment. In this context, foraminifera have been extensively used due to their preservation potential. However, little attention has been paid to the properties of the whole foraminiferal community that, in turn, can be used to depict a comprehensive view of the environment. In this study we focused on the laminated marine sediment core TR17-08 collected in Edisto Inlet (Ross Sea, Antarctica), and the turnover events that characterized the benthic foraminiferal fauna over the last 3.6 kyrs BP. Using the Rate-of-Cehange analysis (RoC), three distinct turnover events were recognised having a long-term effect on the fauna: at 2.7-2.5 kyrs BP, at 1.2-1.0 kyrs BP and at 0.7 kyrs BP. At 2.7-2.5 kyrs BP, ~~a change from a~~ *Miliammina arenacea* disappears and get substituted by different calcareous species, such as ~~to a more prominent presence of~~ *Epistominella exigua, Nonionella iridea* and *Stainforthia feylingi* ~~characterized this transition~~. Aligning with the micropaleontological interpretations, changes in XRF ratios (Zr/Rb; Ca/Ti and Br/Ti) were coeval with the interpretation derived from the RoC and the microfossils assemblage composition. Over this transition, a switch from a multi-year landfast sea-ice (3.6-2.7 kyrs BP) to a seasonal sea-ice dominated environment (2.5-1.2 kyrs BP) was driven by a change in the water mass characteristics, increasing the mCDW (modified Circumpolar Deep Water) content inside the fjord as well as increase the duration of the summer ice-free period. Higher RoC values suggested the absence of a stable benthic foraminifera community ~~over the~~under frequent multi-year landfast sea-ice scenario, while lowest RoC values ~~over~~ during the seasonal sea-ice phase are present, especially ~~over~~ within the 2-1.5 kyrs BP interval, aligning with the macrofaunal response inside the inlet. Continental archives (Penguin and Elephant Seals remains) ~~over~~ along the Victoria Land Coast reported ~~this~~ such a change in the sea-ice type ~~over~~ during the Late Holocene. This study provides further evidence of a change in the sea-ice state ~~over~~ in the Ross Sea after 2.7-2.5 kyrs BP, thus providing further evidence that this water mass intrusion ~~inside~~ onto the continental shelf ~~were higher over~~was more prominent during the 2.5 – 1.2 kyrs BP period, in accordance with persistent summer positive mode of the Southern

Annular Mode. Lastly, this study highlights that using ecological properties of the benthic foraminifera community can be a valuable source of information for high-resolution studies and can provide additional insights into the paleoenvironmental interpretation and paleoclimatic reconstruction that uses benthic foraminiferal species as environmental indicators.

1 Introduction

Unveiling past environmental changes is fundamental to understand the processes that governs the Earth's climate system, and it helps to pinpoint its behaviour in the future. To investigate the past environment, different proxies have been used to obtain a holistic view of all the interacting compartments of the climate system (Strugnell et al., 2022; Toyos et al., 2020; Wang et al., 2023; Wu et al., 2020; Yokoyama et al., 2016). In marine settings, a group that has been extensively used as a tracer for environmental changes are benthic and planktic foraminifera: unicellular marine eukaryotes, with different test material that have a great preservation potential (Sen Gupta, 2003; Murray, 1991, 2006). These organisms inhabit both the surface and bottom water, and they can be used to infer changes in the paleoenvironmental evolution of an area (Sen Gupta, 2003; Murray, 1991, 2006). However, most of the studies that have been carried out with foraminifera focus on comparing changes in the relative abundances of a single species or a group of species and connect them to specific changes in the environment (i.e., Ishman and Sperling, 2002; Kyrmanidou et al., 2018; Majewski et al., 2018).

Community-level (i.e., the whole assemblage considered as one indivisible unit) analysis can help us understand the effects of different environmental phases on the local fauna, while also providing key insight into the environmental evolution (Foster et al., 1990). However, little to no attention has been paid to the properties of the whole community that, potentially, can be used as a reliable tracer to identify significant turnover events linked to the succession of different environmental phases (Hansen et al., 2023; Tomašových and Kidwell, 2010).

In this context, the *Rate-of-Change* (RoC) analysis calculates the compositional changes of a given community through time to extrapolate the rate at which the whole community is changing. This can be used to infer statistically significant changes in the assemblage composition, the so-called Turnover Events (TEs) (Foster et al., 1990; Hansen et al., 2023; Jacobson and Grimm, 1986; Mottl et al., 2021b, a; Shimadzu et al., 2015). The analysis was used by Hansen et al. (2023) on the ecological traits of the benthic foraminifera to infer ecological responses over the western coast of Greenland. This was crucial to understand the consequences of the deglacial-Holocene and the Mid-Holocene warming on the benthic foraminifera fauna in the area, while simultaneously showing that TEs of benthic foraminifera can be linked to climatic perturbation.

In this study, we focus on the marine sediment core TR17-08 from Edisto Inlet (Ross Sea, Antarctica, Fig. 1) with the purpose of understanding short-term (centennial) and long-term (millennial) environmental changes in the area and how they connect with faunal turnover events.

Edisto Inlet is a small basin (16 km long, 4 km wide) located on the northern tip of the Victoria Land in the Ross Sea, characterized by a 110-m thick laminated sedimentary sequence on the bottom, spanning the entire Holocene (Battaglia et al., 2024; Finocchiaro et al., 2005; Di Roberto et al., 2023; Tesi et al., 2020). Previous studies highlighted that environmental

changes occurring in the inlet over the Late Holocene are linked to changes in the global climatic system, as the Medieval Climate Anomaly (MCA, ca. 1.5 – 1.1 kyrs BP) and the Little Ice Age (LIA, ca. 0.7 - 0.1 kyrs BP) (Galli et al., 2023, 2024; Lüning et al., 2019; Mezgec et al., 2017; Stenni et al., 2017; Tesi et al., 2020). In addition, the study of Galli et al., (2024) on ophiuroid ossicles in conjunction with the diversity of the foraminiferal assemblage (Fig. 1c), proposed a shift from an unstable seasonal sea-ice cycle (3.6 – 2.5 kyrs BP) to a stable sea-ice cycle (2.5 - 1.5 kyrs BP), with an optimum of this environmental condition from 2 to 1.5 kyrs BP. The latter has been regarded as the "Ophiuroid Optimum" because of the increase in the probability of occurrence of the ophiuroid *Ophionotus victoriae* and the lowest values of the $IPSO_{25}$ biomarker from the nearby marine sediment core HLF17-01 (Fig. 1c). This geochemical proxy is produced by diatoms that lives inside the sea-ice (sympagic), which are~~is~~ released upon the first break up of the sea-ice (Belt et al., 2016). Due to the dependency of the sea-ice presence of sympagic diatoms to thrive, lower $IPSO_{25}$ concentration have been connected to prolonged periods with an absence of a sea-ice cover (Belt et al., 2016; Massé et al., 2011; Tesi et al., 2020). The transition, occurring around 2.5 kyrs BP, is characterized by a stepwise decrease in the flux and quantity of organic matter content, as testified by the reduction of the Benthic and Planktic Foraminifera Accumulation Rate (BFAR and PFAR, respectively) and by a decrease in the Ice Rafted Debris (IRD) content that suggested the presence of the seasonal sea-ice cover over this period (Galli et al., 2024).

In Edisto Inlet, the depositional regime is governed by the seasonal cycles of landfast sea-ice, a particular type of sea-ice that forms through the freezing of the seawater and by remaining attached to the coast (Fraser et al., 2023). This seasonal behaviour produces the lamination pattern, relating it to the austral summer depositional setting. The first break up of the fjord sea-ice cover happens at the beginning of the austral spring season and leads to the deposition of a dark lamina (Tesi et al., 2020). This type of lamina is characterised by a diatom assemblage dominated by the *Fragilariopsis* genus. On the other hand, prolonged periods of ice-free scenarios lead to the deposition of a white laminae, which are dominated by the diatom *Corethron pennatum*, indicating an oligotrophisation of the upper water column (Tesi et al., 2020). This is also reflected in the biomarker $IPSO_{25}$ (Belt et al., 2016). ~~This geochemical proxy is produced by diatoms that lives inside the sea-ice (sympagic), which is released upon the first break up of the sea-ice. Due to the dependency of the sea-ice presence of sympagic diatoms to thrive, lower $IPSO_{25}$ concentration have been connected to prolonged periods with an absence of a sea-ice cover (Belt et al., 2016; Massé et al., 2011; Tesi et al., 2020).~~ Since most of the depositional signal in the fjord is dominated by the summer season, if the previous interpretation of an unstable-to-stable transition occured, then the rate at which the benthic community is shifting should be higher before the transition, reflecting a period in which a stable community cannot form. In addition, we integrate the results of the RoC with the X-Ray Fluorescence (XRF) data over the last 3.6 kyrs BP, focusing on the 2.5 kyrs BP transition to disentangle the environmental evolution of the area between these two different states.

Thus, the aim of this study is two-fold: 1) connecting the presence of TEs with the presence of significant environmental shifts in the area and, by doing so, unlocking a new objective way of analysing benthic foraminiferal community and 2) reconstructing the paleoenvironmental evolution over the 2.5 kyrs BP transition to understand the relationship between local and regional changes over the study area.

1.1 Study area

The Ross Sea oceanographic circulation is density driven (Fig. 1b): the Antarctic Slope Current (ASC) sits on top of the warmer Circumpolar current (CDW), and both flows westward along the slope. (Orsi and Wiederwohl, 2009; Smith et al., 2012; Whitworth and Orsi, 2006). The CDW can enter the continental shelf when it interacts with the saltier water masses that are flowing from the continent to the open ocean, by reducing the inclination of the isopycnal (Fig. 1b; Budillon et al., 2011; Castagno et al., 2017; Smith et al., 2012). This modified water mass (modified Circumpolar Deep Water, mCDW) enters the continental shelf where it flows southwards, through bathymetric lows (Fig. 1b) (Dinniman et al., 2011; Wang et al., 2023). At the shelf, the inflow of the warmer water masses sustains large persistent ice-free areas, the polynyas (Mathiot et al., 2012; Rusciano et al., 2013). At this point the warm water mass lost its heat and subsides due to the increase in density by salt-rejection processes. As the sea-ice polynya form over the area, katabatic winds move the newly formed sea-ice away from the continent, thus sustaining both the production of the sea-ice, by cooling the sea surface, and the ice-free area (Dale et al., 2017; Drucker et al., 2011). This subsided water mass forms the High Salinity Shelf Water (HSSW), which flows along the same bathymetric lows as the mCDW and arrives at the shelf margin, where it cascades on the seafloor, forming the Antarctic Bottom Water (AABW) (Fig. 1b; Orsi & Wiederwohl, 2009; Wang et al., 2023; Whitworth & Orsi, 2006). Lastly, by studying the current activity in the western part of the Ross Sea, has been noted that the mCDW inflow is mostly seasonal and happens during the austral summer period (Castagno et al., 2017, Wang et al., 2023, Wang et al., 2023).

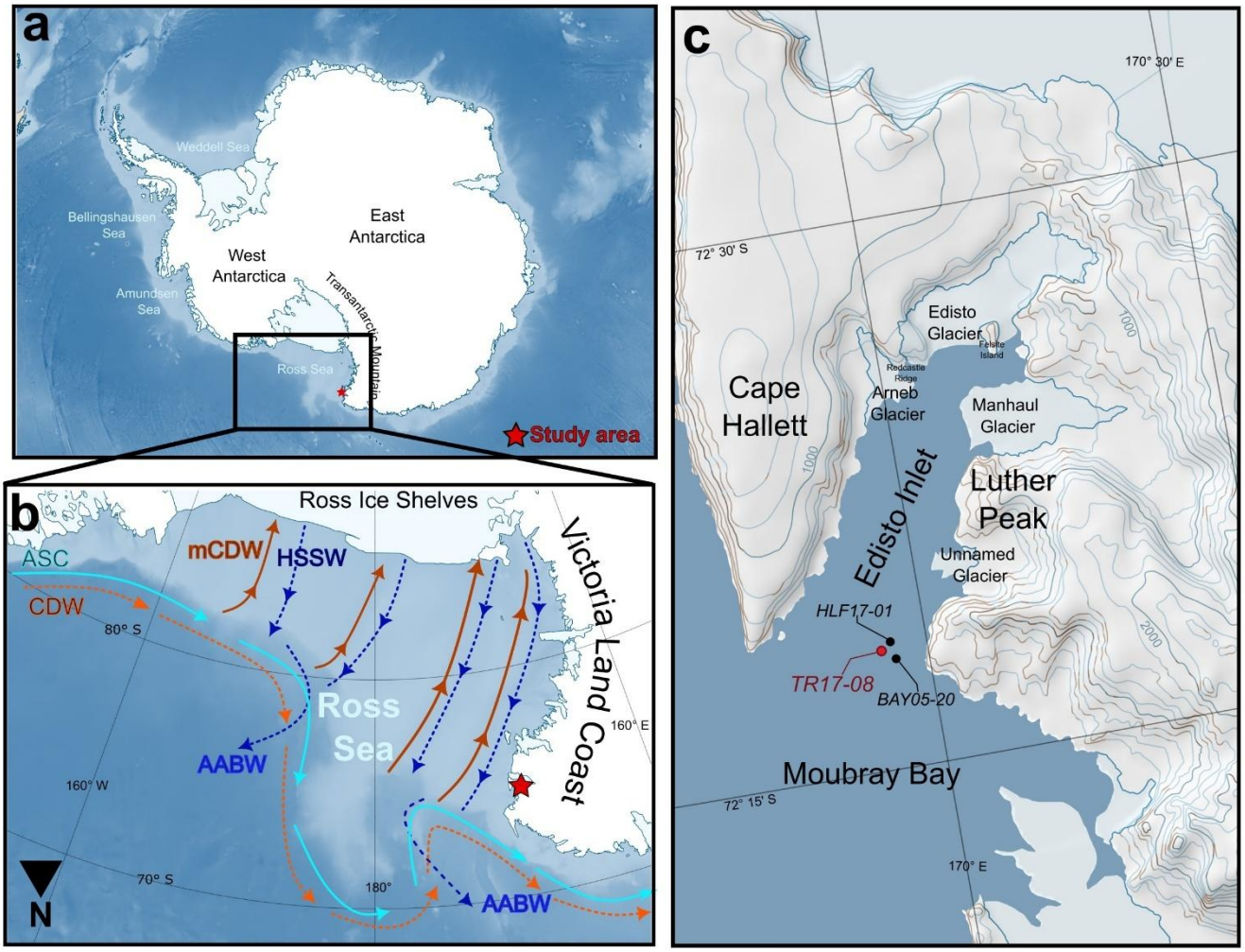

Figure 1.Simplified maps of the study area. a) The location of the study area in Antarctica (red star). b) Main oceanic currents: ASC = Antarctic Slope Current; CDW = Circumpolar Deep Water; mCDW = modified Circumpolar Deep Water; HSSW = High Salinity Shelf Water and AABW = Antarctic Bottom Water. Red colour arrows indicate relatively warm water masses while the cold colour ones indicate the relatively cold-water masses. Solid lines indicate surface water masses, while the dashed ones indicate deeper water masses. The star marks the location of Edisto Inlet. c) Map of Edisto Inlet with analysed marine sediment cores mentioned in this study marked with dots: in red the marine sediment core TR17-08 (this study), while in black the HLF17-01 (Tesi et al., 2020) and the BAY05-20 (Mezgec et al., 2017). The maps are constructed using Quantarctica (Matsuoka et al., 2021)**.**

In particular, Edisto Inlet has an average water depth of 500 m, and the basin is defined by a sill at 400 m depth located at the mouth that divides it from the adjacent Moubray Bay (Fig. 1c). Four local marine terminating glaciers are present: the Arneb Glacier, the Edisto Glacier, the Manhaul Glacier and an unnamed glacier located north of Luther Peak (Fig. 1c). Oceanographic data and CTD profiles from the inner part of the fjord have shown the presence of a double layer stratification of the water column with a pycnocline/thermocline/halocline present at 50-150 m water depth (Battaglia et al., 2024). The

surface layer is fresher and warmer than the deeper one (< -1.8°C). Spatially, the surface waters are saltier (34.27 PSU) and colder (-1.6°C) in the inner part of the fjord respect to the outer ones (Battaglia et al., 2024).

In addition, the presence of sediment drifts at the bottom suggests the presence of relatively long-lived regular bottom water circulation starting at 8 kyrs BP (Battaglia et al., 2024; Finocchiaro et al., 2005).

However, oceanographical data are scarce and for further and more detailed information about the geological and physical settings of the fjord, readers are referred to Battaglia et al., (2024).

2 Methods

To investigate the paleoenvironmental evolution of the Edisto Inlet, the marine sediment core TR17-08 (72° 18.2778′ S; 170° 04.1784′ E; 462 m water depth) was retrieved during the XXXII PNRA (National Italian Program for Antarctic Research) scientific expedition (2016-2017) in the framework of the PNRA project TRACERS (PNRA16_00055). The core, with a length of about 14.5 m, is composed of diatomaceous ooze, with clear distinction between light and dark lamina (Galli et al., 2023, Fig. S1). After a comprehensive reassessment of the age-depth model previously published by Di Roberto et al., (2023), we decided to employ the same model, given its robustness with respect to the application of different radiocarbon calibration curves and marine reservoir ages ~~The age-depth model used is the one proposed by Di Roberto et al., 2023~~ (More information ~~about the age-depth model~~ in the Supplementary Material). The bottom of the core was dated around 3.6 kyrs BP, with an average sedimentation rate of 0.5 cm/yr from 3.6 to 0.7 kyrs BP. Over the last 0.7 kyrs BP, the sedimentation rate diminishes of an order of magnitude, with an average of 0.07 cm/yrs (Di Roberto et al., 2023). Foraminiferal assemblage data, Benthic and Planktic Foraminifera Accumulation Rate (BFAR and PFAR, respectively) as well as IRD (>1 mm) fluxes were used in previous studies to analyse the environmental evolution of the last 2 kyrs BP, as well as to the test the possibilities to use the macrofaunal remains to detect stable environmental conditions (Galli et al., 2023; Galli et al., 2024). Briefly, BFAR and PFAR have been extensively used to detect changes in the organic matter flux to the bottom and the primary productivity regime, respectively (Herguera and Berger, 1991). The IRD flux have been associated to different glacial discharging regime as well as different sea-ice cover regimes, with lower values reflecting less glacial discharge and the presence of a sea-ice cover (Christ et al., 2015; Reeh et al., 1999; Zhou et al., 2021). In this study, we extend the interpretation of the environmental evolution of this area using the micropaleontological data collected by Galli et al., (2024).

2.1 Benthic foraminifera analysis

A TE can be defined as a drastic change in the species composition of a defined area (O'Sullivan et al., 2021; Shimadzu et al., 2015). Over extended periods, TEs can be linked to significant changes in the environmental conditions, providing insights into the extent to which environmental shift can impact a given ecological community, in this case the benthic foraminifera (Foster et al., 1990; Hansen et al., 2023; Mottl et al., 2021b, a). To assess how the evolution of the environment was affecting

the benthic foraminiferal community, we computed and analysed the Rate-of-Change curve (RoC) derived from the changes in relative abundances of the benthic species.

The RoC analysis is a statistical method that computes the significance of a turnover events (TE) in a palaeoecological temporal series in relation to the rate at which the community is changing (Hansen et al., 2023; Jacobson and Grimm, 1986; Mottl et al., 2021b). The analysis is based on the concept of calculating the differences between adjacent stratigraphic levels to identify significant changes in time of the shifts in the biological community (Mottl et al., 2021b, a). These significant changes in time can be detected with several methods: with a linear trend, a nonlinear trend, with the first derivative of the curve or with a signal to noise ratio (Mottl et al., 2021). In our study we compare significant peaks detected by the nonlinear trend method (recommended for paleoecological temporal series) and the significant departure from 0 of the first derivative of the curve (Mottl et al., 2021). The first of the chosen method identifies significant compositional changes as points exceeding a 1.5 standard deviation threshold derived from a fitted non-linear trend (TnL). The second method is based on the first derivative of a fitted Generative Additive Model (GAM derivative method, Gd). The Gd detects a cluster of points when the first derivative of a fitted GAM of the RoC curve is significantly below 0, and it could be used to represent the outcome of a TE (Mottl et al., 2021b, a; Simpson, 2018). These two detection methods can be used to infer significant TEs in a robust way since TnL and Gd are complementary in respect of what they detect (Fig. 2).

The RoC analysis was performed using the *R-Ratepool* package in R using a randomization factor of 10'000, with the recommended setup described in Mottl et al., (2021b). To account for the temporal resolution, we changed the "time standardisation" parameter to 100 and the window was set to 5 to have a similar resolution between the analysis and the sample step of the core (RoC is performed every 20 years). To create the bins used to calculate the differences in the assemblages, we used the "binning with a moving window" approach as described and recommended in Mottl et al. (2021b). To better display the trends of the RoC curve a GAM model (algorithm: REML) was fitted using the *mgcv* package (Simpson, 2018; Wood Simon, 2001).

In addition to analysing the whole period, we also performed the analysis on the 3.6 – 0.7 kyrs BP period, due to the presence of a substantial change in the sedimentation rate (Galli et al., 2023; Di Roberto et al., 2023).

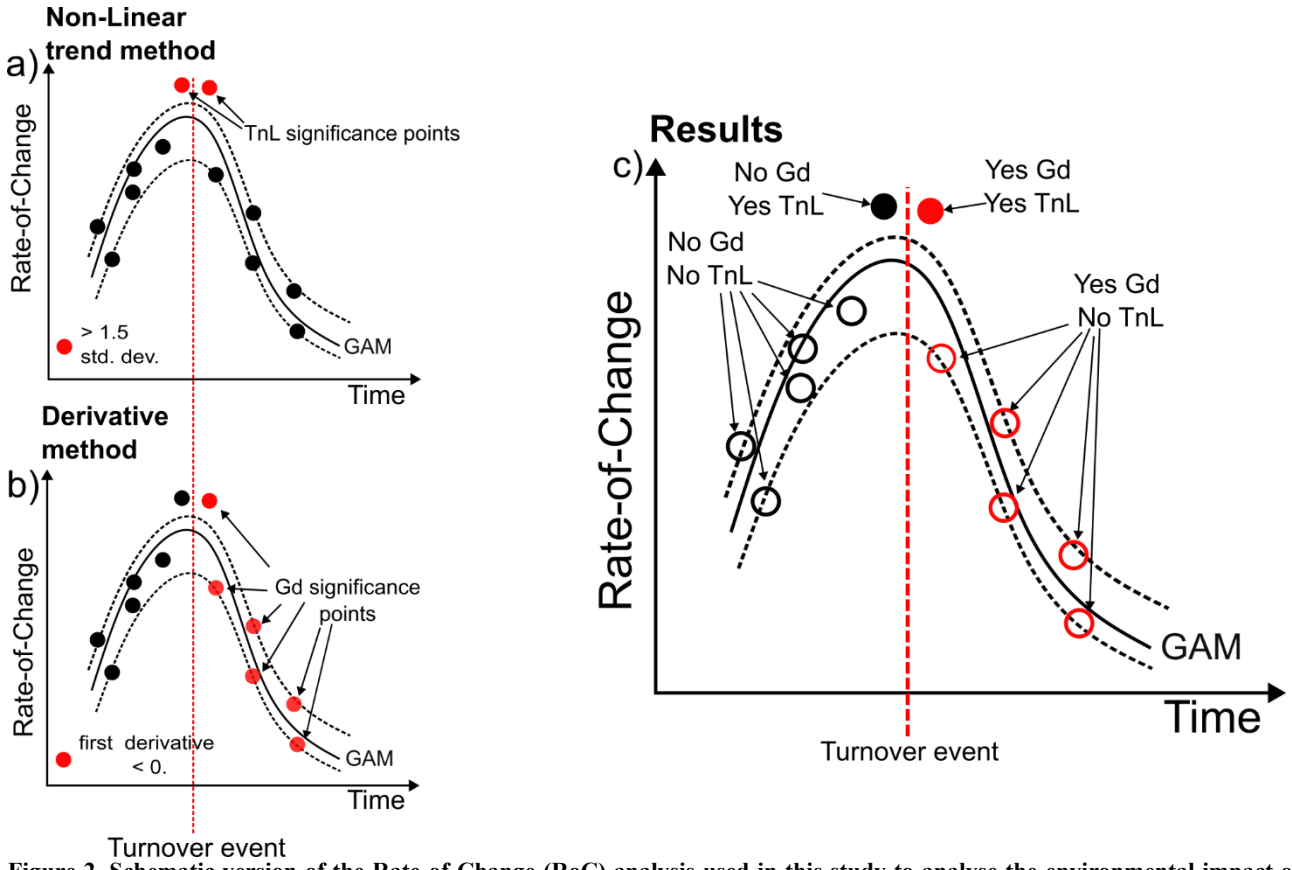

Figure 2. Schematic version of the Rate-of-Change (RoC) analysis used in this study to analyse the environmental impact on the foraminiferal community. a) Non-linear trend detection method (TnL) that relies on points > 1.5 std. dev. of a fitted non-linear trend. b) GAM derivative method (Gd) that relies on the first derivative being < 0. c) End results of the analysis when combined the TnL and the Gd significance points. In this conceptual example, the Turnover Event (red dotted line) is represented as an instantaneous event.

2.24 Sediment properties and lithology

To reconstruct the changes in the sedimentary depositional environment of the study area, a third generation AVAATECH core scanner was used to acquire high-resolution XRF data at 1 cm intervals at the Institute of Marine Sciences at the Italian National Research Council (CNR-ISMAR) of Bologna. The base-10 logarithm of Zr/Rb, Br/Ti and Ca/Ti was used to interpret sedimentary, environmental, and climatic processes as suggested by Croudace & Rothwell (2015). These ratios have been extensively used in paleoenvironmental reconstruction. The Zr/Rb ratio have been used to track changes in the mean-grain size of the silt fraction that can be linked to current strength, with high values reflecting a high current dynamic (Lamy et al., 2024; Wu et al., 2019, 2020). Br/Ti ratio can be used to infer changes in the primary productivity, since Br is related to organic matter of marine origin (Wu et al., 2019; Ziegler et al., 2008), while the Ca/Ti has been used to infer changing in the biogenic

vs. lithogenic sedimentation due to the more prominent presence of Ti in the detrital material and Ca mostly derived from biogenic mineralization (Piva et al., 2008; Taylor et al., 2022). To reduce the noise of these temporal series, a LOESS smoothing curve with a narrow smoothing window (λ=0.1) was fitted using the function *lm* of the base version of R (R Core Team, 2023).

3 Results and discussion

3.1 Turnover events over the last 3.6 kyrs BP in Edisto Inlet

Turnover Events (TEs) were defined only over the benthic foraminiferal community due to the presence of only one planktic species: *Neogloboquadrina pachyderma* (Galli et al., 2024).

The RoC computed for the species composition shows the presence of Gd clusters starting at 3.3 kyrs BP, 2.5 kyrs BP and at 0.7 kyrs BP (Fig. 3a). Of these three Gd clusters, only the latter has both TnL and Gd significance points, reflecting a large environmental shift inferring on the foraminiferal assemblage (1.1 kyrs BP – 0.6 kyrs BP). This can also be inferred by the increase in the RoC at its maximum values (> 0.8, Fig. 3a).

When taking into consideration only the 3.6 - 0.7 kyrs BP period, a cluster of TnL peaks is present at 3.2-3 kyrs BP, at 2.7-2.5 kyrs BP, at 1.2-1 kyrs BP, and a single point at 0.7 kyrs BP (Fig. 3b). The 3.2-3 kyrs BP event is coincident with the presence of a Gd cluster at 3.3-3 kyrs BP (Fig. 3a). Over the 3.6-2.7 kyrs BP period, both RoC curves show no distinctive trend, thus indicating no significant increase or decrease in the compositional change of the benthic foraminiferal community after the 3.3-3 kyrs BP event (Fig. 3). At 2.7-2.5 kyrs BP, TnL points are followed by Gd points (Fig. 3b), with the latter appearing in both analyses (Fig. 3). In contrast to the 3.3-3 kyrs BP, the presence of a visible downward trend of the RoC curves after 2.5 kyrs BP suggest that this event was caused by an environmental shift that had a long-term effect on the fauna (Fig. 3b). The downward trend lasted until 1.8 kyrs BP, while similar values of the RoC from the 3.6-2.7 kyrs BP period are met at 1.5 kyrs BP (Fig. 3b). A presence of a steeper increase starting at 1.5 kyrs BP is also visible in the RoC evaluated on the whole period (Fig. 3a).

Afterwards, several TnL from 1.2 kyrs BP to 1 kyrs BP without being followed by Gd clusters are present, and a peak at 0.7 kyrs BP is reached (Fig. 3). Both the 1.2-1 kyrs BP and the 0.7 kyrs BP points are present over an upward trend (Fig. 3b). Thus, a period that is characterized by a high degree of instability, probably reflecting a transitional period can be inferred (Mottl et al., 2021a). Hence, the period 1.2-1 kyrs BP is connected to a different TE than the one at 0.7 kyrs BP, because of the segregation of the TnL clusters (Fig. 3b). The most recent TnL point (Fig. 3b) is probably caused by substantial environmental shifts occurring at 0.7 kyrs BP. This is highlighted in the RoC computed throughout the whole period, reflected by the presence of both TnL and Gd peak, as well as by reaching the maximum RoC value at that time (Fig. 3a).

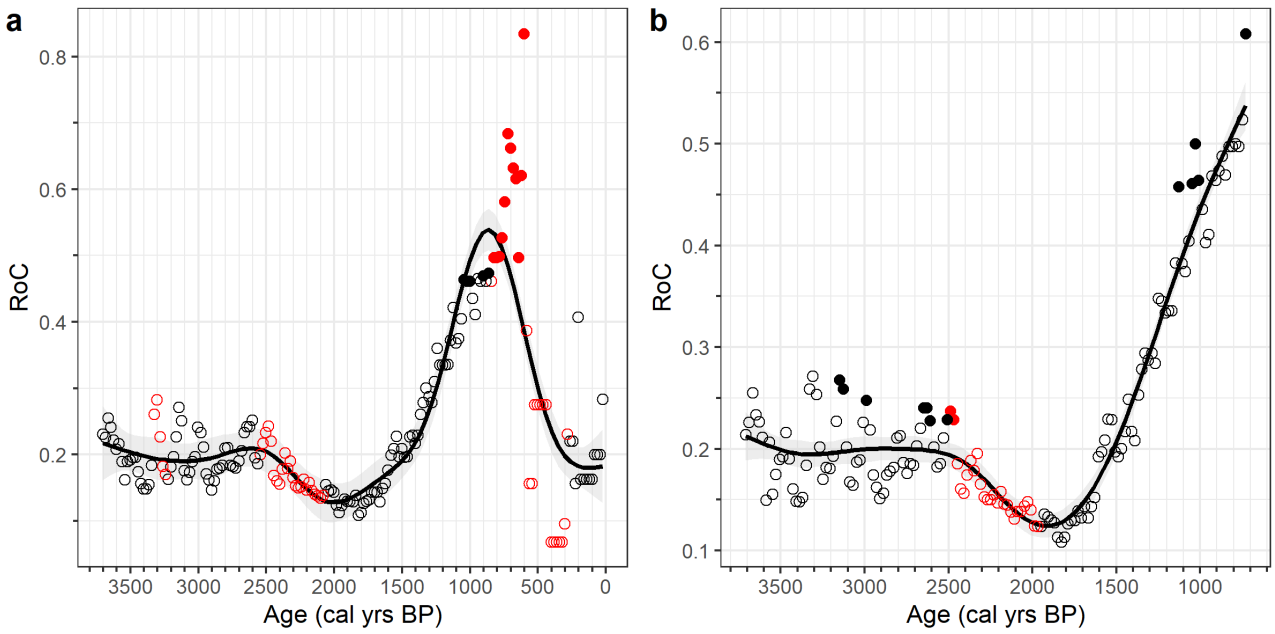

Figure 3. RoC analysis results on the benthic foraminiferal species. a) Results for the whole core; b) results of the analysis evaluated on the 3.6-0.7 kyrs BP. Red colors indicates the significance Gd points, while the black indicates the opposite. Filled circles indicates the significante TnL points. For further information the reader is referred to Fig. 3.

The last 2 kyrs BP were previously investigated for the benthic association, and a succession of different environmental phases was hypothesized (Galli et al., 2023). Over this period, the benthic foraminiferal assemblages were indicative of a seasonal sea-ice phase of the fjord (2-1.5 kyrs BP) followed by a transitional phase (1.5 – 0.7 kyrs BP) while the last 0.7 kyrs BP are indicative of a cold, and almost completely sea-ice covered fjord causing a sharp reduction in the sediment accumulation rate by an order of magnitude (Di Roberto et al., 2023, Tesi et al., 2020). Moreover, the transitional phase of the fjord culminated with a complete switch from a calcareous dominated fauna to an agglutinated dominated one at 1.1 kyrs BP (Galli et al., 2023, Fig. 4). This transition of the dominant test material, coeval with a regional reduction of 2°C over the Victoria Land Region (Stenni et al., 2017). In this context, the RoC analysis agrees with this environmental evolution: lower values of the RoC over the 2-1.5 kyrs BP period are followed by a steeper increase of the compositional changes over the 1.5-0.7 kyrs BP (Fig. 3a). ~~Over~~ During the period of increase instability of the community (increase in the RoC values), the presence of TnL at 1.2-1

kyrs BP, are coeval with the switch in the dominant component of the fauna (Fig 4): During the 2-1.5 kyrs BP interval, the fjord is transitioning from a seasonal sea-ice phase to a completely covered fjord after 1.1 kyrs BP (Galli et al., 2023). Thus, the RoC curve aligns with the evolution of the sea-ice cover duration, with higher ecological instability increasing throughout the last 2 kyrs BP caused by the reduction of the ice-free period.

Following these interpretations, the presence of a difference in the average values of the RoC between 3.6-2.7 kyrs BP and 2.5-1.5 kyrs BP might be indicative of a switch of the state of the sea-ice cover during the summer, from a short ice-free period to a completely ice-free one at 2.7-2.5 kyrs BP. Moreover, the presence of TnL at 3.3-3 kyrs BP are indicative of this ecological instability over the 3.6-2.7 kyrs BP period. On the other hand, lower RoC values and a clear downward trend over the 2.5-1.8 kyrs BP period, suggests a higher ecological stability associated with increasing ice-free conditions over the summer.

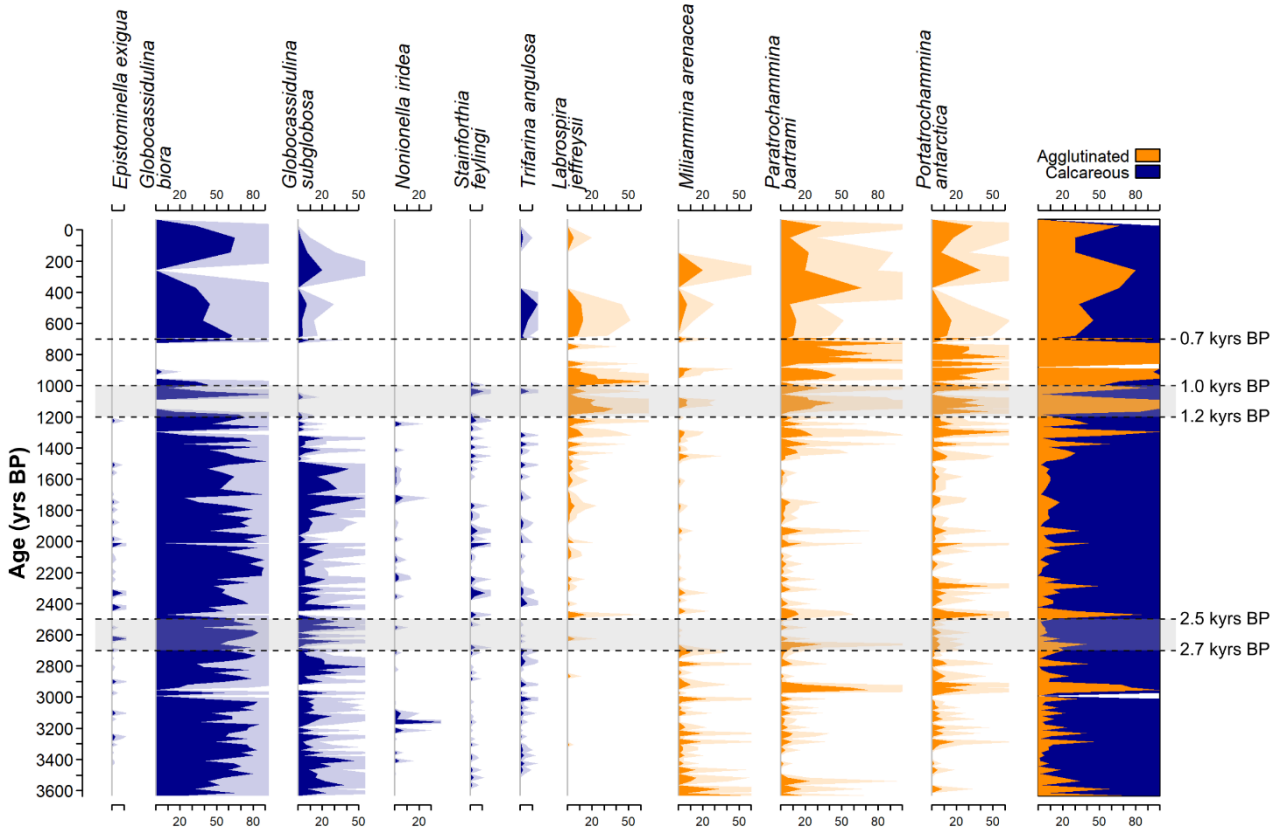

Figure 4. Benthic foraminifera relative abundances of the common species (> 10%) over the last 3.6 kyrs BP, divided as calcareous (blue) and agglutinated species (orange). Black dashed lines and grey area represent temporal locations of the turnover event as defined by the RoC analysis (see the text for further details). On the last panel on the right, the white areas represent barren samples. Shaded areas represent exaggerated silhouettes (x4) to enhance the visibility of the less common species. All plots have the same scaling of the x-axis with one tick indicating a 10% relative abundance.

The benthic foraminiferal species reflect this change in the system state. Throughout the 3.6-1.5 kyrs BP period, the fauna is dominated by calcareous species such as *Globocassidulina biora* and *Globocassidulina subglobosa* (> 50 % of the total

assemblage, Fig. 4). These two common species have been found in Antarctic fjords and sub-ice shelf environments, and have been used as indicator species for high hydrodynamic activities of the bottom water, as well as high input of seasonal organic matter to the sea bottom (Bernhard, 1993; Harloff and Mackensen, 1997; Ishman and Szymcek, 2003; Kyrmanidou et al., 2018; Li et al., 2000; Majewski, 2023; Majewski et al., 2016, 2018; Melis et al., 2021; Sabbatini et al., 2004). In Admiralty Bay (King George Island, Antarctica) specimens belonging to the *Globocassidulina* group are the dominant species of fjord-like environment, even below 400 m water depth, with dead assemblages dominated by *G. biora* specimens (Majewski, 2005, 2010). Hence, the dominance of *G. biora* from the TR17-08 record implies the presence of a fjord-like environment. Agglutinated species such as *Paratrochammina bartrami* and *Portatrochammina antarctica* are also reported as a constituent of fjord-like environments, especially in the > 400 m water depth (Majewski, 2005, 2010). This is also reflected in the TR17-08 record, with both species having low values of relative abundances (< 20%) with isolated peaks from 3.6 to 1.5 kyrs BP, paralleling the interpretation derived from *G. biora* and *G. subglobosa* (Fig. 4).

At 3.1 kyrs BP (> 20%) a peak in the relative abundance of the species *Nonionella iridea* is present (Fig. 4). This species is known to prefer environments that are rich in organic matter and with steep oxygen gradients inside the sediments (Fig. 4, Duffield et al., 2015). Thus, the abrupt increase of *N. iridea* might derive from the presence of a substantial amount of organic matter arriving at the bottom, probably linked to an algal bloom in the surface layer. However, this event had no long-term effect on the benthic assemblage composition as suggested by the RoC curve (Fig. 3), reflecting an anomaly from the natural environment behaviour rather than a systematic change.

The TE occurring at 2.7-2.5 kyrs BP is reflected by the changes in the distribution of the calcareous species *Epistominella exigua, Stainforthia feylingi* and *Trifarina angulosa* along with the almost disappearance of the agglutinated species *Miliammina arenacea* and a sudden increase in the *Portatrochammina antarctica* (Fig. 4).

The agglutinated miliolid *M. arenacea* thrives in environments with high corrosive condition at the bottom and/or where cold and salty water masses are present (Ishman and Szymcek, 2003; Li et al., 2000; Majewski et al., 2018; Murray, 1991). From 3.6 to 2.7 kyrs BP the relative abundance of this species is relatively constant through time (Fig. 4). However, the period following the TE (2.5-1.5 kyrs BP) is characterized by the almost completely disappearance of this species (Fig. 4). This change cannot be ascribed to an increase in the corrosive conditions as carbonate remains the dominant test material throughout the 3.6-1.5 kyrs BP interval (Fig. 4). Thus, the disappearance of *M. arenacea* at 2.7 kyrs BP must be associated to a change in the water masses characteristics.

Even in low percentages, the presence of *E. exigua* in relative higher values during, and after the TE can be indicative of the presence of warmer water masss, as the mCDW in the fjord, and the presence of phytodetritus input from the surface layer (Fig. 5, Harloff & Mackensen, 1997; Ishman & Szymcek, 2003; Majewski et al., 2018; Sabbatini et al., 2004). The more continuous presence of high organic matter indicator species such as *N. iridea* and *S. feylingi*, also suggest an increased flux of organic matter to the bottom (Duffield et al., 2015; Knudsen et al., 2008; Seidenkrantz, 2013; Seidenstein et al., 2018). The overall increase of these species can be caused by the presence of more frequent and prolonged ice-free condition, having the effect of increasing the organic matter delivery to the bottom over the ice-free period, aligning with the RoC curve (Bart et al.,

2018; Majewski and Anderson, 2009; Murray and Pudsey, 2004; Tesi et al., 2020). This is further supported by the sharp increase of *Portatrochammina antarctica*, an agglutinated species sensitive to increases in the primary production (Majewski et al., 2020).

Moreover, species as *Trifarina angulosa* has been used as an indicator of a high energy environment at the bottom, reflecting the presence of bottom water circulation (Ishman and Szymcek, 2003; Melis and Salvi, 2009). Despite being in low percentages, the presence is homogeneous throughout the 3.6-1.5 kyrs BP period, except ~~from~~ during the 2.7-2.5 kyrs BP interval (Fig. 4), reflecting a decrease in the strength of the circulation over this time.

Hence, over the 3.6 – 1.5 kyrs BP interval, from 3.6 to 2.7 kyrs BP, the fjord is characterized by cold and salty bottom water conditions, a bottom water circulation and less primary productivity, with higher RoC values indicating a less ice-free condition over the summer season. At 2.7-2.5 kyrs BP the transition occurs, with the diseapperance of *T. angulosa* suggesting a shutting down of the bottom water circulation. From 2.5 to 1.5 kyrs BP, the benthic fauna suggests more intrusions of mCDW, an increase in both primary productivity and organic matter flux to the sea floor (Fig. 4). The presence of the RoC values over this period suggests the presence of a prolonged period of ice-free conditions over summer.

3.2 Environmental transition at 2.7-2.5 kyrs BP

To have a comprehensive outlook of the environmental transition that characterized Edisto Inlet around 2.7-2.5 kyrs BP, the RoC curves (Fig. 3) and the benthic assemblages (Fig. 4) were compared with the geochemical proxies derived from the TR17-08 sediment core, as well as previously published records from the same core and others derived from nearby marine sediments cores (Fig. 1c, HLF17-01 and Bay05-20c) (Galli et al., 2023, 2024; Mezgec et al., 2017; Tesi et al., 2020). A summary of the interpretations is reported in Table 1.

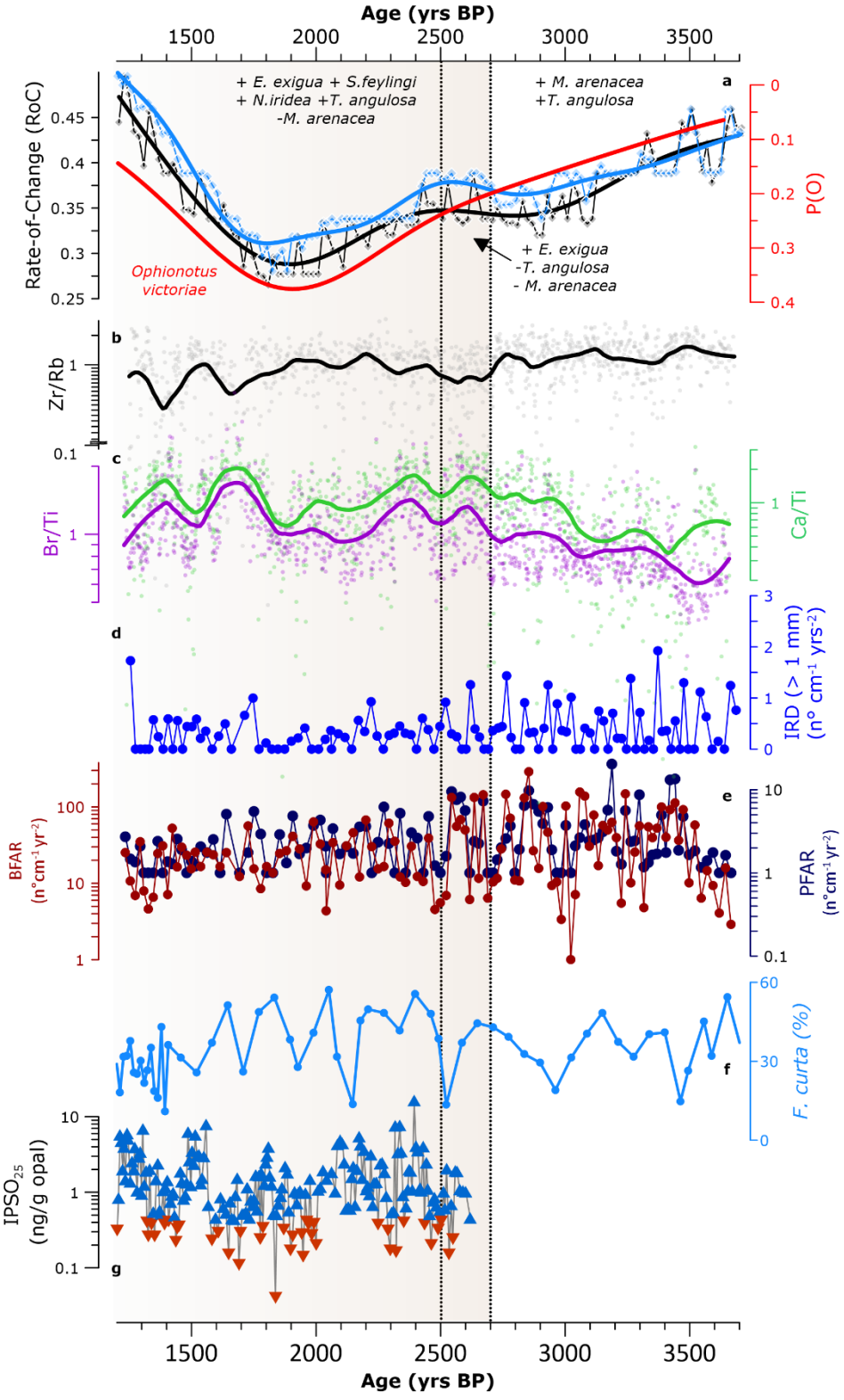
Age (yrs BP)
1500
2000
2500
3000
3500
+ E. exigua + S.feylingi
+ N.iridea +T. angulosa
-M. arenacea
+ M. arenacea
+T. angulosa
a
Rate-of-Change (RoC)
0.45
0.4
0.35
0.3
0.25
P(O)
0
0.1
0.2
0.3
0.4
Ophionotus
victoriae
+ E. exigua
-T. angulosa
- M. arenacea
b
Zr/Rb
1
0.1
c
Br/Ti
1
Ca/Ti
1
d
IRD (> 1 mm)
(n° cm-1 yrs-2)
3
2
1
0
BFAR
(n°cm-1yr-2)
100
10
1
e
PFAR
(n°cm-1yr-2)
10
1
0.1
f
F. curta (%)
60
30
0
IPSO25
(ng/g opal)
10
1
0.1
g
1500
2000
2500
3000
3500
Age (yrs BP)

Figure 5. Paleoenvironmental evolution from 3.6 kyrs BP to 1.5 kyrs BP in Edisto Inlet. Different background colours are used to highlight the transition from a multi-year sea-ice environment to a seasonal sea-ice one. Vertical black dotted lines are indicative of the Turnover Events (TE) at 2.7-2.5 kyrs BP. a) Rate-of-Change (RoC) results (points) and fitted GAM models (line) throughout the core (in black) and for the 0.7-3.6 kyrs BP period (in light blue). The red line indicates the *Ophionotus victoriae* presence modelled as the probability of occurrence using a GAM model (P(O), from Galli et al., 2024). The names indicate the difference benthic foraminiferal species discussed in section 3.1 with + symbol indicating higher abundances and – symbol indicating less presence. b) Logarithm in base 10 of the ratio Zr/Rb (gray dots refers to raw data, blackline represent the fitted LOESS); c) Primary productivity indicators: Ca/Ti (green) and Br/Ti (purple); d) Ice Rafted Debris flux (IRD, blue, from Galli et al., 2024). e) Benthic Foraminifera Accumulation Rate (BFAR, brown) and Planktic Foraminifera Accumulation Rate (PFAR, dark blue, from Galli et al., 2024). The logarithm in base 10 was applied to enhance the visibility of the variability of the fluxes values; f) *Fragilariopsis curta* relative abundance from the core BAY05-20 (from Mezgec et al., 2017). g) $IPSO_{25}$ values in logarithm in base 10 from the HLF17-01 with blue and red triangle indicating different summer sea-ice cover: in red is indicated the ice-free summer, in blue the presence of summer sea-ice cover (threshold values from Tesi et al., 2020)

Over the 3.6 – 2.7 kyrs BP, higher RoC values occur along with the low probability of occurrence of the ophiuroid *Ophionotus victoriae* (P(O), Fig. 5a). Lower values of the P(O) can be associated with unstable seasonal sea-ice conditions due to the dependency of this organism to stable interannual conditions (Fig. 5a, Galli et al., 2024). The benthic foraminiferal assemblage suggests the presence of bottom currents, cold and salty bottom water conditions and low productivity (Fig. 5a). Presence of bottom currents are also suggested by stable values of the Zr/Rb ratio (Fig. 5b), while the low values of both the Ca/Ti and Br/Ti are indicative of a low primary productivity (Fig. 5c) However, in Galli et al. (2024) the high variability of the BFAR and PFAR have been associated to an increase in the organic matter flux to the sea floor with the presence of abrupt increases of primary productivity (Fig. 5d, e), also suggested by the peak of *Nonionella iridea* at 3.1 kyrs BP (Fig. 4). The presence of prolonged periods with multiyear landfast sea-ice could explain these apparent discrepancies between the geochemical and micropaleontological proxy. The present-day setting of Edisto Inlet is mainly controlled by the presence of seasonal landfast sea-ice (Battaglia et al., 2024; Tesi et al., 2020). Landfast sea-ice is prone to become multi-year and can show high nutrient concentrations, since they can be stored and accumulate on the basal portion of the sea-ice for multiple consecutive years. This could lead to an increase in the sea-ice associated diatoms, hence resulting in abrupt increase of the organic matter flux to the bottom upon first break-up (the so called "high nutrient high chlorophyll paradox"; Fraser et al., 2023; Wongpan et al., 2024). Thus, while the surface productivity can be high in a short-time frame due to the presence of algal blooms, as indicated by the BFAR and the PFAR values, this might not have any effect in a longer time frame as shown in the Br/Ti and Ca/Ti ratios because of the prolonged presence of the ice cover (Fig. 5c). In addition, low percentages of *Fragilariopsis curta* from the nearby Bay05-20 sediment core also support this interpretation, since without the presence of a seasonal sea-ice regime, this diatom cannot thrive, explaining the relatively low values in respect to the subsequent phase (Fig. 5f) (Leventer et al., 1993; Mezgec et al., 2017; Waters et al., 2000).

At 2.7-2.5 kyrs BP the TE in the benthic foraminifera highlights the transition from a cold and salty bottom water and low productivity setting to a state in which intrusion of mCDW along with a high primary productivity are present, as suggested by the presence in higher abundance of *E. exigua* and the absence of *M. arenacea* (Fig. 5a). In addition, the absence of *T. angulosa* suggests the absence of a bottom current circulation over this short time interval (Fig. 5a).

These changes in the benthic foraminiferal composition occur in conjunction with a sudden reduction of the Zr/Rb values (Fig. 5b), and a peak in both the Br/Ti and Ca/Ti ratios, aligning with the benthic foraminifera interpretation (Fig. 5c).

The increase in the primary productivity along with the change in the circulation strength, might be related to an increase of the meltwater derived from the marine terminating glaciers. Glacial meltwaters in enclosed basins have the effects of enhancing the mixing of the water column, increasing the nutrient content available in the surface layers (Howe et al., 2010; Pan et al., 2020). However, if the increase in the meltwater content exceeds a certain value, the presence of freshwater can reduce and even shut down the estuarine circulation (Pan et al., 2020).

After the 2.7-2.5 kyrs BP event, the benthic foraminiferal RoC reaches the lowest values reflecting an increasing stability of the summer season (Fig. 5a). This aligns with the macrofaunal response: the P(O) increases to its maximum values, suggesting a stable interannual seasonal sea-ice cycle (Galli et al., 2024). The Zr/Rb ratio is increasing from 2.5 to 1.8 kyrs kyrs BP (Fig. 5b), suggesting a slow restoration of the thermohaline circulation inside the fjord in accordance with the frequent presence of *T. angulosa* (Fig. 4). Both the Ca/Ti and Br/Ti identifies a period characterized by a higher average values in respect to the 3.6-2.7 kyrs BP, suggesting an increase in the primary productivity as well as increase in the organic matter flux to the bottom, consistent with more frequent presence of *N. iridea* and *S .feylingi*, as well as an increase in the *Epistominella exigua* content (Fig. 5a). This species became more frequent over the 2.5-1.5 kyrs BP interval suggesting an increase in the mCDW intrusion inside the inlet (Fig. 4). Intrusion of this warm and nutrient rich water mass can cause the increase in primary productivity as well as a stabilizing the summer condition, promoting prolonged ice-free austral summer (Dinniman et al., 2011; Dale et al., 2017). This aligns with the BFAR and the PFAR record that suggest a more stable input of organic matter in respect to the previous phase (Fig. 5d, Galli et al., 2024). Moreover, the relatively low content of IRD is indicative of prolonged ice-free conditions over the summer season, implying the presence of a seasonal sea-ice cover (Fig. 5d) (Christ et al., 2015; Galli et al., 2024; Peck et al., 2015). In addition, the *Fragilariopsis curta* in core Bay05-20 increases its relative abundances over this period, strengthening the hypothesis of a seasonal sea-ice regime (Allen and Weich, 2022; Leventer et al., 1993; Waters et al., 2000) (Fig. 5f).

Moreover, the period from 2 to 1.5 kyrs BP has been proposed to be the most "stable" in respect to the seasonal sea-ice phase of the fjord due to high P(O) and lowest $IPSO_{25}$ values (Fig. 5a-g, Galli et al., 2024). This is supported by the presence of lowest values of the RoC, indicating the presence of prolonged ice-free period promoting the benthic community stability.

Interval (kyrs BP)	Indicators	Species Presence	Interpretation
3.6-27	↑ IRD; BFAR; PFAR; Zr/Rb; P(O); RoC ↓ *F. curta*; Ca/Ti; Br/Ti	↑ *M. arenacea* and *T. angulosa* ↓ *E. exigua*, *N. iridea, S. feylingi*	Cold and salty bottom water; multi-year sea-ice cover; occurrence of abrupt increases of primary productivity

2.7-2.5	↑ P(O); Zr/Rb. Br/Ti; Ca/Ti; RoC ↓ IRD; BFAR; PFAR;	↑ *E.exigua* ↓ *M. areancea* and *T. angulosa*	Transitional event: intrusion of mCDW and increase in glacier run-off.
2.5-1.5	↑ P(O); Br/Ti; Ca/Ti. - IRD; BFAR; PFAR. ↓ RoC; Zr/Rb; $IPSO_{25}$.	↑ *E.exigua*; *N. iridea, S.feylingi and T. angulosa* ↓ *M. areancea*	Seasonal sea-ice phase with the presence of mCDW and high primary productivity.

Table 1. Summary of Edisto Inlet proxy and environmental succesion over the 3.6-1.5 kyrs BP. Associated with the climatic phase in kyrs BP, a qualitative description of the TR17-08 proxy behaviour (↑= relatively high, ↓= relatively low, - no change), the characteristic benthic foraminfiral species and the schematic environmental phase description. For further detail the readers are referred to the section 3.2 of this manuscript.

3.3 Edisto Inlet as a sentinel for the ocean dynamics in the western Ross Sea over the Late Holocene

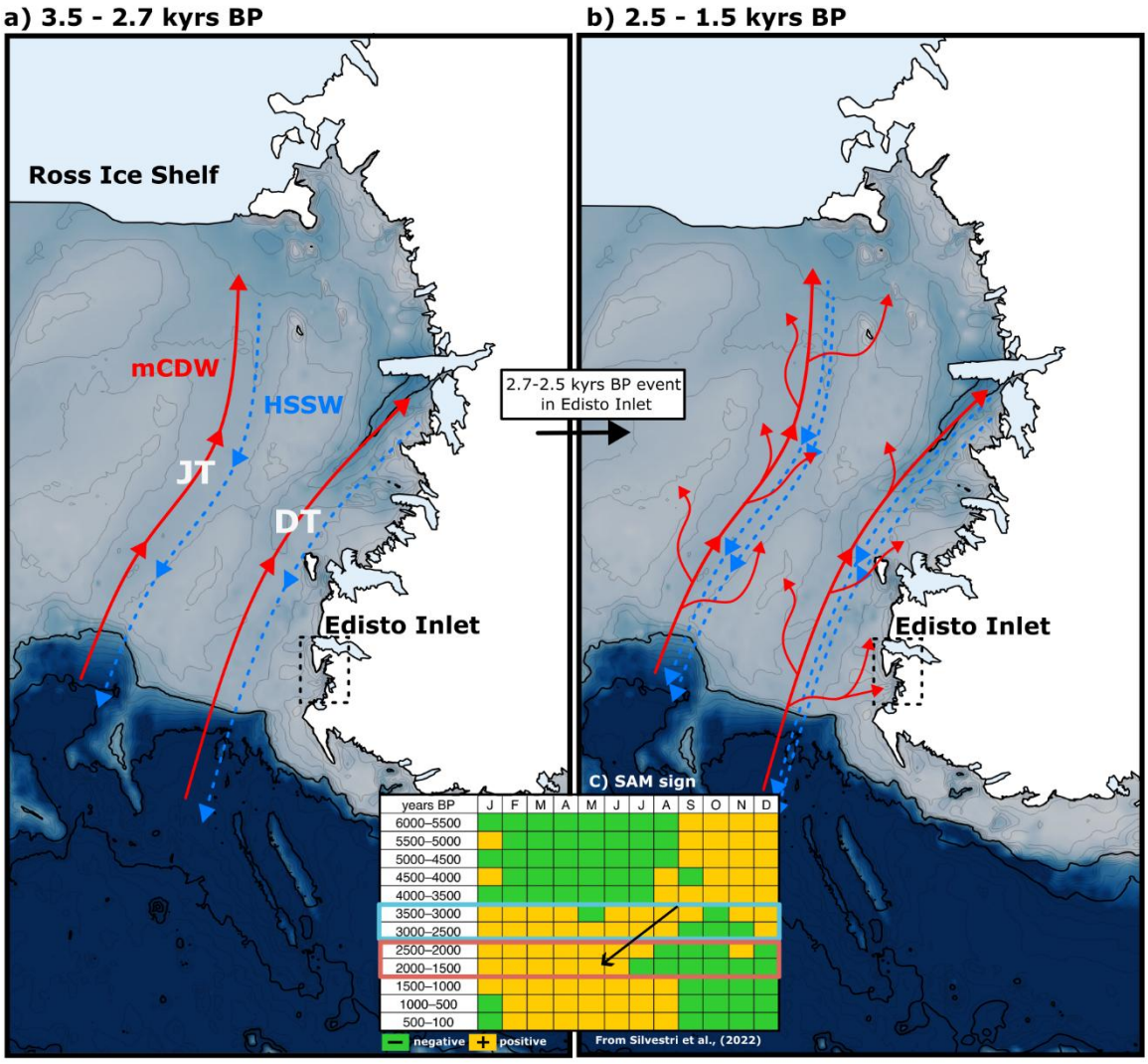

Figure 6. Conceptual regional model of the oceanographic changes in the Ross Sea over the last 3.6 kyrs BP as identified in this study (black dotted square). Red arrows indicate the schematic flows of the superficial mCDW intrusions. Blue arrows indicate the flow of the deeper HSSW. DT= Drygalsky Through, JT = Joides Through. a) oceanographical situation from 3.5 to 2.6 kyrs BP; b) oceanographic circulation from 2.5 to 1.5 kyrs BP; c) Southern Annular Mode values (positive in orange, negative in green) divided by month. The period covered from the panel a) is highlighted by the blue square on the years BP column. The panel b) is highlighted by the red rectangle on the years BP column. The transition is highlighted by the black arrow. Adapted from Silvestri et al. (2022).

Over the Victoria Land Coast, and in general over the Ross Sea, different proxies refer to a similar period as the environmental transition occurring in Edisto Inlet regarding the sea-ice conditions. Hall et al. (2023) studying the distribution of the southern elephant seals (*Mirounga leonina*) remains over the Mid and Late Holocene inferred an increase in the open water conditions, as well as a reduction in the sea-ice presence from 2.3 to 1.8 kyrs BP. They ascribed this ecological dynamic to an increase in

the modified mCDW intrusion over the Victoria Land, having a strong negative effect on the local marine terminating glacier (Hall et al., 2006, 2023).

Another tracer of mCDW intrusion over the Ross Sea is the presence of the Adelie penguin (*Pygoscelis adeliae*) colonies (Hall et al., 2023; Xu et al., 2021). Adelie penguins occupy a different ecological niche than elephant seals despite both relying on the presence of an ice-free zone to feed (Emslie et al., 2003, 2018; Hall et al., 2006). Since Penguins rely on the presence of a consolidated ice platform to breed, while the elephant seals do not, due to the increased number of penguins colonies ("Penguin Optimum", 4.6 -2.8 kyrs) followed by an increase number of southern elephant seals colonies ("Southern elephant seals optimum", 2.3-1.8 kyrs BP), Hall et al. (2023) inferred that over the 5-2.7 kyrs BP, the coastal Victoria Land region was a landfast ice dominated environment, while, from 2.5 kyrs BP to 0.5 kyrs BP, a period of warmer-than- present climate ~~onset~~ occurred that may be related to a strengthening of the mCDW intrusion. The 2.5-0.5 kyrs BP interval was also associated with prolonged ice-free conditions.

The switch in the sea-ice conditions over the Victoria Land region is coeval with the TE occurring ~~i~~on the benthic foraminifera community at 2.7-2.5 kyrs BP (Hall et al., 2023). This local transition might be linked to an increas~~ed~~ing regional intrusion of mCDW over the western coast of the Ross Sea (Fig. 6). An addition of the overall content of mCDW could 1) sustain the free-ice period; 2) increase the glacial input derived from the melting of the marine terminating glacier and 3) enhance the primary productivity, due to the high nutrient concentration that this water mass has (Arrigo and van Dijken, 2004; Dale et al., 2017; Dinniman et al., 2011; Emslie et al., 2003; Hall et al., 2006; Mathiot et al., 2012; Orsi and Wiederwohl, 2009; Smith et al., 2012; Smith and Gordon, 1997; Wang et al., 2023; Xu et al., 2021). Over the transition period, the intensification of glacier run-off would have promoted the thawing of the marine terminating glaciers and increasing the meltwater content. This has the effect of reducing the circulation inside the inlet, thus implying a stronger influence of the mCDW over the study area.

In addition, the presence of mCDW inside the inlet is reasonable due to the bathymetric distribution that this water mass has over the Ross Sea region. The mCDW is generally found at depth of around 200-400 m and, within the Drygalski through, this water mass flows southward, being consistent with the morphological features that characterized the inlet (Castagno et al., 2017; Orsi and Wiederwohl, 2009; Smith Jr. et al., 2014; Wang et al., 2023; Zhang et al., 2024). Since this should be a regional response, another key element is the presence of a relation between the upwelling of CDW onto the continental shelf and a positive phase of the Southern Annular Mode (SAM, fig. 6c). The SAM is defined as a latitudinal gradient of sea-level pressure between mid and high latitude (Fogt and Marshall, 2020; Marshall, 2003). Positive phases of this atmospheric modes are associated with the strengthening and the poleward movement of the westerlies, that, in turns, increases the upwelling of the CDW onto the continental shelf and the production of the HSSW while simultaneously enhancing the polynya efficiency (Campbell et al., 2019; Gordon et al., 2007; Zhang et al., 2024). In a simulation using state-of-the-art models, Silvestri et al. (2022), showed an increase in the positive phases of the SAM in the austral summer over the 2.5-1.5 kyrs BP interval (Fig. 6c) that is consistent with the transition that characterized the Edisto Inlet sea-ice regime (Fig. 6c). A shift from more prolonged and positive SAM condition over the summer period is present throughout 2.5-1.5 kyrs BP, causing more prominent mCDW

intrusions over Victoria Land Coast, ultimately causing more intrusions of this water mass inside the inlet, sustaining the ice-free season (Fig. 6).

This is also consistent with the study of ~~-~~Mezgec et al., (2017) that compared marine and ice core records. In their study, increases in the of the polynya efficiency along with an increase in the katabatic wind regimes was hypothesized starting around 2.5 kyrs BP, which is coeval with our record.

All these observations suggests that TE of the benthic foraminifera in Edisto Inlet are related to the sea-ice cover variations that, ultimately, are connected to regional oceanographic and atmospheric changes, thus providing an exceptional record that offers high-resolution insight about the environmental changes over the Victoria Land Coast.

4 Conclusion

In this study we analysed the environmental shifts inferred on the Edisto Inlet by looking at the Rate-of-Change (RoC) of the benthic foraminiferal assemblage to infer significant environmental shifts. We showed that the RoC could bear relevant information for paleoenvironmental reconstruction. Four different Turnover Events (TE) i~~o~~n the benthic foraminiferal community were recognised: 3.3-3.1 kyrs BP, 2.5-2.7 kyrs BP, 1.2 – 1.0 kyrs BP and 0.7 kyrs BP. While the first one did not have any long-term effect on the faunal composition, the other three TE were caused by major environmental changes that had long-term effect on the faunal composition. In Edisto Inlet, changes in the RoC values are indicative different sea-ice cover regimes. Of particular interest, the TE at 2.7-2.5 kyrs BP was caused by a transition from a multi-year sea-ice dominated environment (3.6-2.7 kyrs BP) to a seasonal sea-ice dominated one (2.5-1.5 kyrs BP). The presence of this change in the sea-ice type in the fjord had the effect of increasing the stability of the benthic community, resulting in more stable community over the seasonal sea-ice phase. The loss of *Miliammina arenacea* and *Trifarina angulosa* in conjunction with increases in *Epistominella exigua* suggested more intrusion of mCDW (modified Circumpolar Deep Water) over the 2.5-1.2 kyrs BP period. XRF ratio (Zr/Rb, Br/Ti and Ca/Ti) showed a good agreement with the benthic record, demonstrating the potentiality of using RoC analysis in paleoenvironmental studies to identify important faunal changes that are connected to environmental transitions. By looking at a more regional setting, the seasonal sea-ice phase (2.5-1.5 kyrs BP) is coeval with the changes~~ing~~ inferred~~ing~~ over the Victoria Land Coast, with a similar type of sea-ice change occurring over the same interval. The presence of positive summer phases of the Southern Annular Mode during this period strengthens this view, with more upwelling of CDW onto the shelf and increasing polynya efficiency.

Lastly, we highlight the importance that Edisto Inlet might have to study regional oceanographical changes over the Ross Sea region, implying that the local environmental transitions that this site experiences can be used as sentinel for regional changing over the Victoria Land Region. Thus, the presence of this high-resolution record could offer key insights on the Holocene environmental evolution over the Ross Sea.

5 Data availability

All the data used in this study are included in the supplementary material of this article.

6 Author contributions

GG: conceptualization, formal analysis, investigation, visualization, writing the original draft and preparation; KHH: formal analysis, investigation, validation; AdR, FG and PG: data curation; AdR and KG: Funding acquisition. All authors contributed to the reviewing and editing process.

7 Competing interests

The authors declare that they have no conflict of interests.

8 Acknowledgemnts

We thank the sorting centre of MNA – Trieste (Italy) for the sediment core samples, and the CNR-ISMAR section of Bologna (Italy) for the XRF core scanning analysis and data. We also thank all the staff of the *Italica*, and the dr. Leonardo Langone for his contributions to sample campaign and the radiocarbon dating. Lastly, we would like to thank the anonymous reviewers and the editor for the suggestions and comments that substantially improved the manuscript.

9 Financial supports

This research has been supported by the Ministero dell'Università e della Ricerca (projects EDISTHO (grant no. PNRA 2018_00010) and TRACERS (grant no. PNRA2016A3/00055)).

10 References

Allen, C. S. and Weich, Z. C.: Variety and Distribution of Diatom-Based Sea Ice Proxies in Antarctic Marine Sediments of the Past 2000 Years, Geosciences (Basel), 12, 282, https://doi.org/10.3390/geosciences12080282, 2022.

Arrigo, K. R. and van Dijken, G. L.: Annual changes in sea-ice, chlorophyll a, and primary production in the Ross Sea, Antarctica, Deep Sea Research Part II: Topical Studies in Oceanography, 51, 117–138, https://doi.org/10.1016/j.dsr2.2003.04.003, 2004.

Bart, P. J., DeCesare, M., Rosenheim, B. E., Majewski, W., and McGlannan, A.: A centuries-long delay between a paleo-ice-shelf collapse and grounding-line retreat in the Whales Deep Basin, eastern Ross Sea, Antarctica, Sci Rep, 8, 12392, https://doi.org/10.1038/s41598-018-29911-8, 2018.

Battaglia, F., De Santis, L., Baradello, L., Colizza, E., Rebesco, M., Kovacevic, V., Ursella, L., Bensi, M., Accettella, D., Morelli, D., Corradi, N., Falco, P., Krauzig, N., Colleoni, F., Gordini, E., Caburlotto, A., Langone, L., and Finocchiaro, F.: The discovery of the southernmost ultra-high-resolution Holocene paleoclimate sedimentary record in Antarctica, Mar Geol, 467, 107189, https://doi.org/10.1016/j.margeo.2023.107189, 2024.

Belt, S. T., Smik, L., Brown, T. A., Kim, J. H., Rowland, S. J., Allen, C. S., Gal, J. K., Shin, K. H., Lee, J. I., and Taylor, K. W.: Source identification and distribution reveals the potential of the geochemical Antarctic sea ice proxy IPSO25, Nat Commun, 7, 12655, https://doi.org/10.1038/ncomms12655, 2016.

Bernhard, J. M.: Experimental and field evidence of Antarctic foraminiferal tolerance to anoxia and hydrogen sulfide, Mar Micropaleontol, 20, 203–213, https://doi.org/10.1016/0377-8398(93)90033-T, 1993.

Budillon, G., Castagno, P., Aliani, S., Spezie, G., and Padman, L.: Thermohaline variability and Antarctic bottom water formation at the Ross Sea shelf break, Deep Sea Research Part I: Oceanographic Research Papers, 58, 1002–1018, https://doi.org/10.1016/j.dsr.2011.07.002, 2011.

Campbell, E. C., Wilson, E. A., Moore, G. W. K., Riser, S. C., Brayton, C. E., Mazloff, M. R., and Talley, L. D.: Antarctic offshore polynyas linked to Southern Hemisphere climate anomalies, Nature, 570, 319–325, https://doi.org/10.1038/s41586-019-1294-0, 2019.

Capotondi, L., Bergami, C., Giglio, F., Langone, L., and Ravaioli, M.: Benthic foraminifera distribution in the Ross Sea (Antarctica) and its relationship to oceanography, Bollettino della Società Paleontologica Italiana, 57, 187–202, https://doi.org/10.4435/BSPI.2018.12, 2018.

Capotondi, L., Bonomo, S., Budillon, G., Giordano, P., and Langone, L.: Living and dead benthic foraminiferal distribution in two areas of the Ross Sea (Antarctica), Rend Lincei Sci Fis Nat, 31, 1037–1053, https://doi.org/10.1007/s12210-020-00949-z, 2020.

Castagno, P., Falco, P., Dinniman, M. S., Spezie, G., and Budillon, G.: Temporal variability of the Circumpolar Deep Water inflow onto the Ross Sea continental shelf, Journal of Marine Systems, 166, 37–49, https://doi.org/10.1016/j.jmarsys.2016.05.006, 2017.

Christ, A. J., Talaia-Murray, M., Elking, N., Domack, E. W., Leventer, A., Lavoie, C., Brachfeld, S., Yoo, K. C., Gilbert, R., Jeong, S. M., Petrushak, S., Wellner, J., Balco, G., Brachfeld, S., de Batist, M., Domack, E., Gordon, A., Haran, A., Henriet, J. P., Huber, B., Ishman, S., Jeong, S., King, M., Lavoie, C., Leventer, A., McCormick, M., Mosley-Thompson, E., Pettit, E., Scambos, T., Smith, C., Thompson, L., Truffer, M., van Dover, C., Vernet, M., Wellner, J., Yu, K., and Zagorodnov, V.: Late Holocene glacial advance and ice shelf growth in Barilari Bay, Graham Land, West Antarctic Peninsula, Bulletin of the Geological Society of America, 127, 297–315, https://doi.org/10.1130/B31035.1, 2015.

Dale, E. R., McDonald, A. J., Coggins, J. H. J., and Rack, W.: Atmospheric forcing of sea ice anomalies in the Ross Sea polynya region, Cryosphere, 11, 267–280, https://doi.org/10.5194/tc-11-267-2017, 2017.

Dinniman, M. S., Klinck, J. M., and Smith, W. O.: A model study of Circumpolar Deep Water on the West Antarctic Peninsula and Ross Sea continental shelves, Deep Sea Res 2 Top Stud Oceanogr, 58, 1508–1523, https://doi.org/10.1016/j.dsr2.2010.11.013, 2011.

Drucker, R., Martin, S., and Kwok, R.: Sea ice production and export from coastal polynyas in the Weddell and Ross Seas, Geophys Res Lett, 38, n/a-n/a, https://doi.org/10.1029/2011gl048668, 2011.

Duffield, C. J., Hess, S., Norling, K., and Alve, E.: The response of Nonionella iridea and other benthic foraminifera to "fresh" organic matter enrichment and physical disturbance, Mar Micropaleontol, 120, 20–30, https://doi.org/10.1016/j.marmicro.2015.08.002, 2015.

Emslie, S. D., Berkman, P. A., Ainley, D. G., Coats, L., and Polito, M.: Late-Holocene initiation of ice-free ecosystems in the southern Ross Sea, Antarctica, Mar Ecol Prog Ser, 262, 19–25, https://doi.org/10.3354/meps262019, 2003.

Emslie, S. D., McKenzie, A., and Patterson, W. P.: The rise and fall of an ancient adélie penguin 'supercolony' at cape adare, antarctica, R Soc Open Sci, 5, https://doi.org/10.1098/rsos.172032, 2018.

Finocchiaro, F., Langone, L., Colizza, E., Fontolan, G., Giglio, F., and Tuzzi, E.: Record of the early Holocene warming in a laminated sediment core from Cape Hallett Bay (Northern Victoria Land, Antarctica), Glob Planet Change, 45, 193–206, https://doi.org/10.1016/j.gloplacha.2004.09.003, 2005.

Fogt, R. L. and Marshall, G. J.: The Southern Annular Mode: Variability, trends, and climate impacts across the Southern Hemisphere, https://doi.org/10.1002/wcc.652, 1 July 2020.

Foster, D. R., KSchoonmaker, P., and Pickett, S. T. A.: Insights from paleoecology to community ecology, Trends Ecol Evol, 5, 119–122, https://doi.org/10.1016/0169-5347(90)90166-B, 1990.

Fraser, A. D., Wongpan, P., Langhorne, P. J., Klekociuk, A. R., Kusahara, K., Lannuzel, D., Massom, R. A., Meiners, K. M., Swadling, K. M., Atwater, D. P., Brett, G. M., Corkill, M., Dalman, L. A., Fiddes, S., Granata, A., Guglielmo, L., Heil, P., Leonard, G. H., Mahoney, A. R., McMinn, A., van der Merwe, P., Weldrick, C. K., and Wienecke, B.: Antarctic Landfast Sea Ice: A Review of Its Physics, Biogeochemistry and Ecology, https://doi.org/10.1029/2022RG000770, 1 June 2023.

Galli, G., Morigi, C., Melis, R., Di Roberto, A., Tesi, T., Torricella, F., Langone, L., Giordano, P., Colizza, E., Capotondi, L., Gallerani, A., and Gariboldi, K.: Paleoenvironmental changes related to the variations of the sea-ice cover during the Late Holocene in an Antarctic fjord (Edisto Inlet, Ross Sea) inferred by foraminiferal association, J Micropalaeontol, 42, 95–115, https://doi.org/10.5194/jm-42-95-2023, 2023.

Galli, G., Morigi, C., Thuy, B., and Gariboldi, K.: Late Holocene echinoderm assemblages can serve as paleoenvironmental tracers in an Antarctic fjord, Sci Rep, 14, https://doi.org/10.1038/s41598-024-66151-5, 2024.

Gordon, A. L., Visbeck, M., and Comiso, J. C.: A Possible Link between the Weddell Polynya and the Southern Annular Mode*, J Clim, 20, 2558–2571, https://doi.org/10.1175/JCLI4046.1, 2007.

Grange, L. J., Tyler, P. A., Peck, L., and Cornelius, N.: Long-term interannual cycles of the gametogenic ecology of the Antarctic brittle star Ophionotus victoriae, Mar Ecol Prog Ser, 278, 14–155, https://doi.org/10.3354/meps278141, 2004.

Sen Gupta, B. K.: Modern Foraminifera, Springer Netherlands, Dordrecht, https://doi.org/10.1007/0-306-48104-9, 2003.

Hall, B. L., Hoelzel, A. R., Baroni, C., Denton, G. H., Le Boeuf, B. J., Overturf, B., and Topf, A. L.: Holocene elephant seal distribution implies warmer-than-present climate in the Ross Sea, PNAS, 103, 10213–10217, https://doi.org/10.1073/pnas.0604002103, 2006.

Hall, B. L., Koch, P. L., Baroni, C., Salvatore, M. C., Hoelzel, A. R., de Bruyn, M., and Welch, A. J.: Widespread southern elephant seal occupation of the Victoria land coast implies a warmer-than-present Ross Sea in the mid-to-late Holocene, Quat Sci Rev, 303, https://doi.org/10.1016/j.quascirev.2023.107991, 2023.

Hansen, K. E., Pearce, C., and Seidenkrantz, M. S.: Response of Arctic benthic foraminiferal traits to past environmental changes, Sci Rep, 13, https://doi.org/10.1038/s41598-023-47603-w, 2023.

Harloff, J. and Mackensen, A.: Recent benthic foraminiferal associations and ecology of the Scotia Sea and Argentin Basin, Mar Micropaleontol, 31, 1–29, https://doi.org/10.1016/S0377-8398(96)00059-X, 1997.

Herguera, J. C. and Berger, W. H.: Paleoproductivity from benthic foraminifera abundance: Glacial to postglacial change in the west-equatorial Pacific, Geology, 19, 1173–1176, https://doi.org/10.1130/0091-7613(1991)019<1173:PFBFAG>2.3.CO;2, 1991.

Howe, J. A., Austin, W. E. N., Forwick, M., Paetzel, M., Harland, R., and Cage, A. G.: Fjord systems and archives: a review, Geological Society, London, Special Publications, 344, 5–15, https://doi.org/10.1144/sp344.2, 2010.

Ishman, S. E. and Sperling, M. R.: Benthic foraminiferal record of Holocene deep-water evolution in the Palmer Deep, western Antarctica Peninsula, Geology, 30, 435–438, https://doi.org/10.1130/0091-7613(2002)030<0435:BFROHD>2.0.CO;2, 2002.

Ishman, S. E. and Szymcek, P.: Foraminiferal Distributions in the Former Larsen-A Ice Shelf and Prince Gustav Channel Region, Eastern Antarctic Peninsula Margin: A Baseline for Holocene Paleoenvironmental Change, in: Antarctic Peninsula Climate Variability: Historical and Paleoenvironmental Perspectives, 239–260, https://doi.org/10.1029/AR079p0239, 2003.

Jacobson, G. L. and Grimm, E. C.: A Numerical Analysis of Holocene Forest and Prairie Vegetation in Central Minnesota, Ecology, 67, 958–966, https://doi.org/10.2307/1939818, 1986.

Knudsen, K. L., Stabell, B., Seidenkrantz, M.-S., EirÍKsson, J. Ó. N., and Blake, W.: Deglacial and Holocene conditions in northernmost Baffin Bay: sediments, foraminifera, diatoms and stable isotopes, Boreas, 37, 346–376, https://doi.org/10.1111/j.1502-3885.2008.00035.x, 2008.

Kyrmanidou, A., Vadman, K. J., Ishman, S. E., Leventer, A., Brachfeld, S., Domack, E. W., and Wellner, J. S.: Late Holocene oceanographic and climatic variability recorded by the Perseverance Drift, northwestern Weddell Sea, based on benthic foraminifera and diatoms, Mar Micropaleontol, 141, 10–22, https://doi.org/10.1016/j.marmicro.2018.03.001, 2018.

Lamy, F., Winckler, G., Arz, H. W., Farmer, J. R., Gottschalk, J., Lembke-Jene, L., Middleton, J. L., van der Does, M., Tiedemann, R., Alvarez Zarikian, C., Basak, C., Brombacher, A., Dumm, L., Esper, O. M., Herbert, L. C., Iwasaki, S.,

Kreps, G., Lawson, V. J., Lo, L., Malinverno, E., Martinez-Garcia, A., Michel, E., Moretti, S., Moy, C. M., Ravelo, A. C., Riesselman, C. R., Saavedra-Pellitero, M., Sadatzki, H., Seo, I., Singh, R. K., Smith, R. A., Souza, A. L., Stoner, J. S., Toyos, M., de Oliveira, I. M. V. P., Wan, S., Wu, S., and Zhao, X.: Five million years of Antarctic Circumpolar Current strength variability, Nature, 627, 789–796, https://doi.org/10.1038/s41586-024-07143-3, 2024.

Leventer, A., Dunbar, R. B., and DeMaster, D. J.: Diatom evidence for Late Holocene climatic events in Granite Harbor, Antarctica, Paleoceanography, 8, 373–386, https://doi.org/10.1029/93PA00561, 1993.

Li, B., Yoon, H., and Park, B.: Foraminiferal assemblages and CaCO3 dissolution since the last deglaciation in the Maxwell Bay, King George Island, Antarctica, Mar Geol, 169, 239–257, https://doi.org/10.1016/S0025-3227(00)00059-1, 2000.

Lüning, S., Gałka, M., and Vahrenholt, F.: The Medieval Climate Anomaly in Antarctica, Palaeogeogr Palaeoclimatol Palaeoecol, 532, https://doi.org/10.1016/j.palaeo.2019.109251, 2019.

Majewski, W.: Benthic foraminiferal communities: distribution and ecology in Admiralty Bay, King George Island, West Antarctica, Pol Polar Res, 26, 159–214, 2005.

Majewski, W.: Benthic foraminifera from West Antarctic fiord environments: An overview, Pol Polar Res, 31, 61–82, https://doi.org/10.4202/ppres.2010.05, 2010.

Majewski, W.: Supplement of Unique benthic foraminiferal communities (stained) in diverse environments of sub-Antarctic fjords, South Georgia, 20, 523–544, https://doi.org/10.5194/bg-20-523-2023-supplement, 2023.

Majewski, W. and Anderson, J. B.: Holocene foraminiferal assemblages from Firth of Tay, Antarctic Peninsula: Paleoclimate implications, Mar Micropaleontol, 73, 135–147, https://doi.org/10.1016/j.marmicro.2009.08.003, 2009.

Majewski, W., Wellner, J. S., and Anderson, J. B.: Environmental connotations of benthic foraminiferal assemblages from coastal West Antarctica, Mar Micropaleontol, 124, 1–15, https://doi.org/10.1016/j.marmicro.2016.01.002, 2016.

Majewski, W., Bart, P. J., and McGlannan, A. J.: Foraminiferal assemblages from ice-proximal paleo-settings in the Whales Deep Basin, eastern Ross Sea, Antarctica, Palaeogeogr Palaeoclimatol Palaeoecol, 493, 64–81, https://doi.org/10.1016/j.palaeo.2017.12.041, 2018.

Marshall, G. J.: Trends in the Southern Annular Mode from observations and reanalyses, J Clim, 16, 4134–4143, https://doi.org/https://doi.org/10.1175/1520-0442(2003)016<4134:TITSAM>2.0.CO;2, 2003.

Massé, G., Belt, S. T., Crosta, X., Schmidt, S., Snape, I., Thomas, D. N., and Rowland, S. J.: Highly branched isoprenoids as proxies for variable sea ice conditions in the Southern Ocean, Antarct Sci, 23, 487–498, https://doi.org/10.1017/s0954102011000381, 2011.

Mathiot, P., Jourdain, N. C., Barnier, B., Gallée, H., Molines, J. M., Le Sommer, J., and Penduff, T.: Sensitivity of coastal polynyas and high-salinity shelf water production in the Ross Sea, Antarctica, to the atmospheric forcing, Ocean Dyn, 62, 701–723, https://doi.org/10.1007/s10236-012-0531-y, 2012.

Matsuoka, K., Skoglund, A., Roth, G., de Pomereu, J., Griffiths, H., Headland, R., Herried, B., Katsumata, K., Le Brocq, A., Licht, K., Morgan, F., Neff, P. D., Ritz, C., Scheinert, M., Tamura, T., Van de Putte, A., van den Broeke, M., von

Deschwanden, A., Deschamps-Berger, C., Van Liefferinge, B., Tronstad, S., and Melvær, Y.: Quantarctica, an integrated mapping environment for Antarctica, the Southern Ocean, and sub-Antarctic islands, Environmental Modelling & Software, 140, https://doi.org/10.1016/j.envsoft.2021.105015, 2021.

Melis, R. and Salvi, G.: Late Quaternary foraminiferal assemblages from western Ross Sea (Antarctica) in relation to the main glacial and marine lithofacies, Mar Micropaleontol, 70, 39–53, https://doi.org/10.1016/j.marmicro.2008.10.003, 2009.

Melis, R., Capotondi, L., Torricella, F., Ferretti, P., Geniram, A., Hong, J. K., Kuhn, G., Khim, B.-K., Kim, S., Malinverno, E., Yoo, K. C., and Colizza, E.: Last Glacial Maximum to Holocene paleoceanography of the northwestern Ross Sea inferred from sediment core geochemistry and micropaleontology at Hallett Ridge, J Micropalaeontol, 40, 15–35, https://doi.org/10.5194/jm-40-15-2021, 2021.

Mezgec, K., Stenni, B., Crosta, X., Masson-Delmotte, V., Baroni, C., Braida, M., Ciardini, V., Colizza, E., Melis, R., Salvatore, M. C., Severi, M., Scarchilli, C., Traversi, R., Udisti, R., and Frezzotti, M.: Holocene sea ice variability driven by wind and polynya efficiency in the Ross Sea, Nat Commun, 8, 1334, https://doi.org/10.1038/s41467-017-01455-x, 2017.

Mottl, O., Flantua, S. G. A., Bhatta, K. P., Felde, V. A., Giesecke, T., Goring, S., Grimm, E. C., Haberle, S., Hooghiemstra, H., Ivory, S., Kuneš, P., Wolters, S., Seddon, A. W. R., and Williams, J. W.: Global acceleration in rates of vegetation change over the past 18,000 years, Science (1979), 372, 860–864, https://doi.org/10.1126/science.abg1685, 2021a.

Mottl, O., Grytnes, J. A., Seddon, A. W. R., Steinbauer, M. J., Bhatta, K. P., Felde, V. A., Flantua, S. G. A., and Birks, H. J. B.: Rate-of-change analysis in paleoecology revisited: A new approach, Rev Palaeobot Palynol, 293, https://doi.org/10.1016/j.revpalbo.2021.104483, 2021b.

Murray, J. W.: Ecology and palaeoecology of benthic foraminifera, Routledge, 1991.

Murray, J. W.: Ecology and Applications of Benthic Foraminifera, Cambridge University Press, https://doi.org/10.1017/CBO9780511535529, 2006.

Murray, J. W. and Pudsey, C. J.: Living (stained) and dead foraminifera from the newly ice-free Larsen Ice Shelf, Weddell Sea, Antarctica: Ecology and taphonomy, Mar Micropaleontol, 53, 67–81, https://doi.org/10.1016/j.marmicro.2004.04.001, 2004.

Orsi, A. H. and Wiederwohl, C. L.: A recount of Ross Sea waters, Deep Sea Research Part II: Topical Studies in Oceanography, 56, 778–795, https://doi.org/10.1016/j.dsr2.2008.10.033, 2009.

O'Sullivan, J. D., Terry, J. C. D., and Rossberg, A. G.: Intrinsic ecological dynamics drive biodiversity turnover in model metacommunities, Nat Commun, 12, https://doi.org/10.1038/s41467-021-23769-7, 2021.

Pan, B. J., Vernet, M., Manck, L., Forsch, K., Ekern, L., Mascioni, M., Barbeau, K. A., Almandoz, G. O., and Orona, A. J.: Environmental drivers of phytoplankton taxonomic composition in an Antarctic fjord, Prog Oceanogr, 183, https://doi.org/10.1016/j.pocean.2020.102295, 2020.

Peck, V. L., Allen, C. S., Kender, S., McClymont, E. L., and Hodgson, D. A.: Oceanographic variability on the West Antarctic Peninsula during the Holocene and the influence of upper circumpolar deep water, Quat Sci Rev, 119, 54–65, https://doi.org/10.1016/j.quascirev.2015.04.002, 2015.

Piva, A., Asioli, A., Schneider, R. R., Trincardi, F., Andersen, N., Colmenero-Hidalgo, E., Dennielou, B., Flores, J. A., and Vigliotti, L.: Climatic cycles as expressed in sediments of the PROMESSI borehole PRAD1-2, central Adriatic, for the last 370 ka: 1. Integrated stratigraphy, Geochemistry, Geophysics, Geosystems, 9, https://doi.org/10.1029/2007GC001713, 2008.

Reeh, N., Mayer, C., Miller, H., Thomsen, H. H., and Weidick, A.: Present and past climate control on fjord glaciations in Greenland: Implications for IRD-deposition in the sea, Geophys Res Lett, 26, 1039–1042, https://doi.org/10.1029/1999GL900065, 1999.

Di Roberto, A., Colizza, E., Del Carlo, P., Petrelli, M., Finocchiaro, F., and Kuhn, G.: First marine cryptotephra in Antarctica found in sediments of the western Ross Sea correlates with englacial tephras and climate records, Sci Rep, 9, 10628, https://doi.org/10.1038/s41598-019-47188-3, 2019.

Di Roberto, A., Re, G., Scateni, B., Petrelli, M., Tesi, T., Capotondi, L., Morigi, C., Galli, G., Colizza, E., Melis, R., Torricella, F., Giordano, P., Giglio, F., Gallerani, A., and Gariboldi, K.: Cryptotephras in the marine sediment record of the Edisto Inlet, Ross Sea: Implications for the volcanology and tephrochronology of northern Victoria Land, Antarctica, Quaternary Science Advances, 10, https://doi.org/10.1016/j.qsa.2023.100079, 2023.

Rusciano, E., Budillon, G., Fusco, G., and Spezie, G.: Evidence of atmosphere–sea ice–ocean coupling in the Terra Nova Bay polynya (Ross Sea—Antarctica), Cont Shelf Res, 61–62, 112–124, https://doi.org/10.1016/j.csr.2013.04.002, 2013.

Sabbatini, A., Morigi, C., Ravaioli, M., and Negri, A.: Abyssal benthic foraminifera in the Polar Front region (Pacific sector): Faunal composition, standing stock and size structure, Chemistry and Ecology, 20, S117–S129, https://doi.org/10.1080/02757540410001655387, 2004.

Seidenkrantz, M.-S.: Benthic foraminifera as palaeo sea-ice indicators in the subarctic realm – examples from the Labrador Sea–Baffin Bay region, Quat Sci Rev, 79, 135–144, https://doi.org/10.1016/j.quascirev.2013.03.014, 2013.

Seidenstein, J. L., Cronin, T. M., Gemery, L., Keigwin, L. D., Pearce, C., Jakobsson, M., Coxall, H. K., Wei, E. A., and Driscoll, N. W.: Late Holocene paleoceanography in the Chukchi and Beaufort Seas, Arctic Ocean, based on benthic foraminifera and ostracodes, arktos, 4, 1–17, https://doi.org/10.1007/s41063-018-0058-7, 2018.

Shimadzu, H., Dornelas, M., and Magurran, A. E.: Measuring temporal turnover in ecological communities, Methods Ecol Evol, 6, 1384–1394, https://doi.org/10.1111/2041-210X.12438, 2015.

Silvestri, G., Berman, A. L., Braconnot, P., and Marti, O.: Long-term trends in the Southern Annular Mode from transient Mid- to Late Holocene simulation with the IPSL-CM5A2 climate model, Clim Dyn, 59, 903–914, https://doi.org/10.1007/s00382-022-06160-0, 2022.

Simpson, G. L.: Modelling palaeoecological time series using generalised additive models, Front Ecol Evol, 6, https://doi.org/10.3389/fevo.2018.00149, 2018.

Smith Jr., W. O., Ainley, D. G., Arrigo, K. R., and Dinniman, M. S.: The oceanography and ecology of the Ross Sea, Ann Rev Mar Sci, 6, 469–487, https://doi.org/10.1146/annurev-marine-010213-135114, 2014.

Smith, W., Sedwick, P., Arrigo, K., Ainley, D., and Orsi, A.: The Ross Sea in a Sea of Change, Oceanography, 25, 90–103, https://doi.org/10.5670/oceanog.2012.80, 2012.

Smith, W. O. and Gordon, L. I.: Hyperproductivity of the Ross Sea (Antarctica) polynya during austral spring, Geophys Res Lett, 24, 233–236, https://doi.org/10.1029/96gl03926, 1997.

Stenni, B., Curran, M. A. J., Abram, N. J., Orsi, A., Goursaud, S., Masson-Delmotte, V., Neukom, R., Goosse, H., Divine, D., van Ommen, T., Steig, E. J., Dixon, D. A., Thomas, E. R., Bertler, N. A. N., Isaksson, E., Ekaykin, A., Werner, M., and Frezzotti, M.: Antarctic climate variability on regional and continental scales over the last 2000 years, Climate of the Past, 13, 1609–1634, https://doi.org/10.5194/cp-13-1609-2017, 2017.

Strugnell, J. M., McGregor, H. V., Wilson, N. G., Meredith, K. T., Chown, S. L., Lau, S. C. Y., Robinson, S. A., and Saunders, K. M.: Emerging biological archives can reveal ecological and climatic change in Antarctica, https://doi.org/10.1111/gcb.16356, 1 November 2022.

Taylor, S. P., Patterson, M. O., Lam, A. R., Jones, H., Woodard, S. C., Habicht, M. H., Thomas, E. K., and Grant, G. R.: Expanded North Pacific Subtropical Gyre and Heterodyne Expression During the Mid-Pleistocene, Paleoceanogr Paleoclimatol, 37, https://doi.org/10.1029/2021PA004395, 2022.

Tesi, T., Belt, S. T., Gariboldi, K., Muschitiello, F., Smik, L., Finocchiaro, F., Giglio, F., Colizza, E., Gazzurra, G., Giordano, P., Morigi, C., Capotondi, L., Nogarotto, A., Köseoğlu, D., Di Roberto, A., Gallerani, A., and Langone, L.: Resolving sea ice dynamics in the north-western Ross Sea during the last 2.6 ka: From seasonal to millennial timescales, Quat Sci Rev, 237, https://doi.org/10.1016/j.quascirev.2020.106299, 2020.

Tomašových, A. and Kidwell, S. M.: The effects of temporal resolution on species turnover and on testing metacommunity models, American Naturalist, 175, 587–606, https://doi.org/10.1086/651661, 2010.

Toyos, M. H., Lamy, F., Lange, C. B., Lembke-Jene, L., Saavedra-Pellitero, M., Esper, O., and Arz, H. W.: Antarctic Circumpolar Current Dynamics at the Pacific Entrance to the Drake Passage Over the Past 1.3 Million Years, Paleoceanogr Paleoclimatol, 35, https://doi.org/10.1029/2019pa003773, 2020.

Wang, Y., Zhou, M., Zhang, Z., and Dinniman, M. S.: Seasonal variations in Circumpolar Deep Water intrusions into the Ross Sea continental shelf, Front Mar Sci, 10, https://doi.org/10.3389/fmars.2023.1020791, 2023.

Waters, R. L., van den Enden, R., and Marchant, H. J.: Summer microbial ecology off East Antarctica (80–150°E): protistan community structure and bacterial abundance, Deep Sea Research Part II: Topical Studies in Oceanography, 47, 2401–2435, https://doi.org/10.1016/S0967-0645(00)00030-8, 2000.

Whitworth, T. and Orsi, A. H.: Antarctic Bottom Water production and export by tides in the Ross Sea, Geophys Res Lett, 33, https://doi.org/10.1029/2006gl026357, 2006.

Wongpan, P., Meiners, K. M., Vancoppenolle, M., Fraser, A. D., Moreau, S., Saenz, B. T., Swadling, K. M., and Lannuzel, D.: Gross Primary Production of Antarctic Landfast Sea Ice: A Model-Based Estimate, J Geophys Res Oceans, 129, https://doi.org/10.1029/2024JC021348, 2024.

Wood Simon: mgcv: GAMs and generalized ridfe regression for R, R news, 1, 20–25, 2001.

Wu, L., Wang, R., Krijgsman, W., Chen, Z., Xiao, W., Ge, S., and Wu, J.: Deciphering Color Reflectance Data of a 520-kyr Sediment Core From the Southern Ocean: Method Application and Paleoenvironmental Implications, Geochemistry, Geophysics, Geosystems, 20, 2808–2826, https://doi.org/10.1029/2019GC008212, 2019.

Wu, L., Wilson, D. J., Wang, R., Yin, X., Chen, Z., Xiao, W., and Huang, M.: Evaluating Zr/Rb Ratio From XRF Scanning as an Indicator of Grain-Size Variations of Glaciomarine Sediments in the Southern Ocean, Geochemistry, Geophysics, Geosystems, 21, https://doi.org/10.1029/2020GC009350, 2020.

Xu, Q. B., Yang, L. J., Gao, Y. S., Sun, L. G., and Xie, Z. Q.: 6,000-Year Reconstruction of Modified Circumpolar Deep Water Intrusion and Its Effects on Sea Ice and Penguin in the Ross Sea, Geophys Res Lett, 48, https://doi.org/10.1029/2021GL094545, 2021.

Yokoyama, Y., Anderson, J. B., Yamane, M., Simkins, L. M., Miyairi, Y., Yamazaki, T., Koizumi, M., Suga, H., Kusahara, K., Prothro, L., Hasumi, H., Southon, J. R., and Ohkouchi, N.: Widespread collapse of the Ross Ice Shelf during the late Holocene, Proc Natl Acad Sci U S A, 113, 2354–2359, https://doi.org/10.1073/pnas.1516908113, 2016.

Zhang, Z., Xie, C., Castagno, P., England, M. H., Wang, X., Dinniman, M. S., Silvano, A., Wang, C., Zhou, L., Li, X., Zhou, M., and Budillon, G.: Evidence for large-scale climate forcing of dense shelf water variability in the Ross Sea, Nat Commun, 15, 8190, https://doi.org/10.1038/s41467-024-52524-x, 2024.

Zhou, Y., McManus, J. F., Jacobel, A. W., Costa, K. M., Wang, S., and Alvarez Caraveo, B.: Enhanced iceberg discharge in the western North Atlantic during all Heinrich events of the last glaciation, Earth Planet Sci Lett, 564, https://doi.org/10.1016/j.epsl.2021.116910, 2021.

Ziegler, M., Jilbert, T., De Lange, G. J., Lourens, L. J., and Reichart, G. J.: Bromine counts from XRF scanning as an estimate of the marine organic carbon content of sediment cores, Geochemistry, Geophysics, Geosystems, 9, https://doi.org/10.1029/2007GC001932, 2008.